United Nations Educational, Scientific and Cultural Organization
Geothermal Training Programme Under the auspices of UNESCO

GRÓ GTP, Grensásvegur 9,
IS-108 Reykjavík, Iceland

Reports 2021
Number 30

# DESALINATION OF GEOTHERMAL WATER USING A MULTISTAGE FLASH DISTILLATION SYSTEM AND SOLAR ENERGY

**Kriti Yadav**
Centre of Excellence for Geothermal Energy
Pandit Deendayal Energy University
Raisan, Gandhinagar-382007
GUJARAT, INDIA
*kriti.yphd15@spt.pdpu.ac.in*

## ABSTRACT

Dholera is a region in W-India with scarcity of fresh drinking water. As it is situated nearby the sea even the groundwater is saline in nature. Geothermal water is also found at shallow depth in most places. Hence, access to potable drinking water is difficult there. The objective of this study is to develop a green desalination system which can provide potable fresh drinking water. In this study, a Multi-Stage Flash Distillation system (MSF system) using solar energy was designed for desalination of geothermal water. To fulfil the temperature requirement of the MSF system, solar Evacuated Tubes (ETC) are used to increase the water temperature in the system. This paper provides an overview of the tectonic setting of Dholera, the region's stratigraphy, and geochemistry of the area. It also reviews several types of desalination systems and solar collector characteristics. Python programming and thermodynamic properties from the CoolProp library were used for the design and thermodynamic analysis of the whole system including both the ETC and the MSF desalination. Simulations were performed for the heat production with the ETC and the geothermal MSF system generating steam and salt. The details of material selection and corrosion protection techniques are also reviewed in this paper. The results of the simulation were satisfactory, and according to them the salt concentration of the water could be reduced to the standards of freshwater, i.e. below 1000 ppm. A cost estimation of the system was also performed in the form of CAPEX and OPEX expenditures.

## 1. INTRODUCTION

The scarcity of freshwater supplies is an undeniable issue in today's civilization. Potable water scarcity seems to have become a limiting factor to human development in many places throughout the world since it is a prerequisite for human existence (Liu and Su, 2007). The global need for desalination is growing in tandem with the advancement of industrial technologies, the rapid growth of the global population and increasing living standards (Zhang, 2008; Bremere et al., 2001). Desalination facilities currently generate nearly 95 million $m^3$ of water per day, with the Middle East and North Africa (MENA) province accounting for 48 percent of the world total desalination capacity (Caldera and Breyer, 2017; Jones et al., 2019). The utilization of reverse osmosis (RO), electrodialysis (ED), multi-effect distillation (MED), and multi-stage flash (MSF) procedures have received a lot of attention in

recent years due to their role in increasing the availability and security of freshwater plant operations. Among them, MSF desalination is an important technology in the desalination industry due to its high reliability and good distillate quality. However, its manufacturing costs are considerably high and the device's performance is influenced significantly by factors such as seawater and geothermal water temperature, as well as fouling factor for the equipment (Zhao et al., 2017; Wang et al., 2014). As a result, it is of importance to develop methods that reduce the MSF distillation device's operational costs.

Desalination technologies combined with renewable energy sources such as solar, geothermal, and wind have enormous potential for future potable water supply in dry areas (Mahmoudi et al., 2010; Mahmoudi et al., 2008). A successful combination of these technologies could enable countries to address water scarcity issues using a local source of energy, which does not cause pollution or makes a significant contribution to climate change. As the demand for fossil fuel is increasing and the supply is limited, the fiscal outlay for renewable desalination systems is increasing steadily. This is also due to a wide range of potential pairings of renewable energy sources and desalination systems (Rodriguez et al., 1996; European Geothermal Energy Council, 2010). The Multiple-effect desalination system is still one of the most common and successful desalination equipment (Al-Hallaj et al., 1998). To boost relative water content productivity and enhance system efficiency, residual heat of condensation is collected in two or even more phases. Deeper knowledge of the thermodynamic principles underpinning the many uses of residual heat of condensation inside a multi-effect humidifying-dehumidifying solar energy system is critical to improve product performance (Al-Hallaj et al., 1998). Furthermore, while a technology may be effective and efficient, it might not be cost-effective (Fath, 1998). As a result, when selecting a desalination system, both energy efficiency and economics must be considered. It has also been seen that small desalination systems can provide the quality and quantity of freshwater required in remote areas with lack of good infrastructure.

The Royal Navy first used desalination in the late 18th century to improve navigation liberty by storing additional water on the battleships (Rognoni et al., 2010). Because ships had steam engines at that time, the earliest desalination technology was a single flash distillation which has evolved over time into the more successful MSF. Desalination facilities were built in Qatar and Kuwait in the year 1953. In Qatar, five such devices with an installed output of 682 $m^3$/day were installed, and 10 such MSF units with an installed output of 4550 $m^3$/day were constructed in Kuwait. In Shuwaikh, ten additional units of the same capacity were constructed in 1955. Desalination facilities grew in popularity around the globe after this, with businesses like Krupp in Germany, Westinghouse in the United States, and SIR (Società Italiana Resine) in Italy emerging (Ragnoni et al., 2010).

Another widely used method is reverse osmosis (RO) which uses semipermeable membranes. Water is extracted from a pressurized brine solution by passing it through water-permeable membranes. The differential pressure between the pressurized source water and the atmosphere encourages the permeable fluid to pass through the membrane. The phenomenon of osmosis was originally recognized in 1748 by Jean-Antoine Nollet, but went unnoticed for nearly two centuries (Amio Water Treatment Ltd., 2021). The earliest experiments were initiated in 1956 by the scholars Sidney Loeb at the University of California and Srinivasa Sourirajan at the University of Florida. The very first membrane was developed in 1959, and the first plant, with a throughput of 19 $m^3$/day, was erected in 1965 (Ragnoni, 2010). The invention of asymmetrical membranes, which have a varied permeability, improved this approach by allowing more water to flow through (Amio Water Treatment Ltd., 2021). The slow spread of the RO technology was originally attributed to the high electricity consumption compared to other methods, as well as the short life of semi - permeable membranes (Ragnoni, 2010). Because brackish water has a lower solute concentration than seawater, the earliest uses were focused on that.

Presently, RO is the most widely used technology, followed by MSF and Multi-Effect Distillation (MED). In 2018, most of the installed capacity of desalination facilities was based on these three techniques as seen in Figure 1; RO (68.7%), MSF (17.6%), and MED (17.6%). Other techniques like humidification-dehumidification, pervaporation, microbial desalination, forward osmosis, adsorption

desorption desalination, etc. play a minor role (6.8%) (Jones et al., 2019). Desalination facilities can be found throughout the world, although they are most common in the Middle East and North Africa (47.5 percent of global capacity) (Jones et al., 2019). Several methods are now being investigated with the goal of lowering energy requirements for freshwater production.

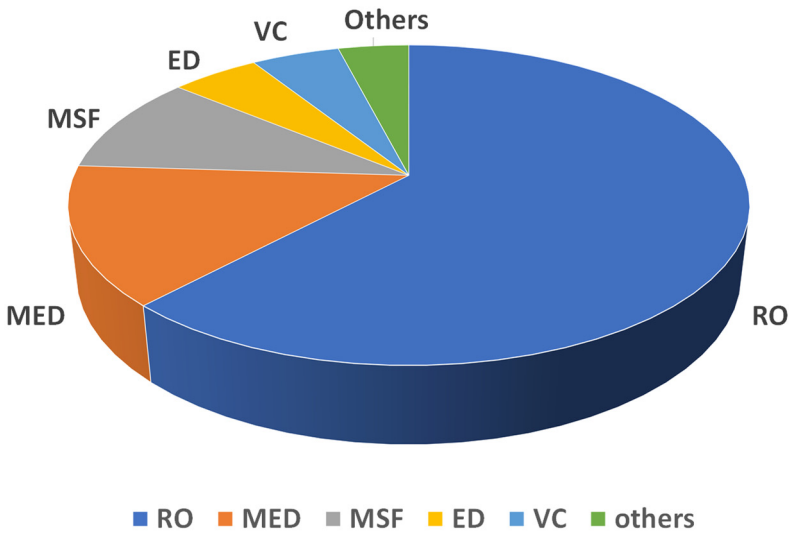


FIGURE 1: Installed percentage of desalination systems worldwide (Jones et al., 2019). RO = reverse osmosis, MED = multi-effect distillation, MSF = multi-stage flash, ED = electrodialysis and VC = vapour compression.

The objective of this study is to design a sustainable and green desalination system to desalinate geothermal water in Dholera, Gujarat, W-India. The geothermal water in the region is located at very shallow depth and, hence, it occurs when drilling for groundwater takes place. A Multi-Stage Flash (MSF) Distillation system is designed using python programming. The reason to choose a MSF system was to produce freshwater of high quality with very low salt concentration. This plant can be used for two purposes, that is, for freshwater production and for salt production from the discharged brine. The aim was also to make the whole system sustainable and green, hence, the solar evacuated tubes act as the energy source. The selection of solar collectors was based on the temperature requirement for the MSF system. This system will be able to fulfil the need of the locals for drinking water and will also produce salt. In addition, the rejected heat from the system can be used for other purposes like food drying, balneology etc.

## 2. BACKGROUND OF THE STUDY AREA

### 2.1 Geological settings and description of study area

The state of Gujarat, located in the western part of India, is bounded by the ocean on three sides. The coastline of the state is around 1,600 km long, most of it lies around the Kathiawar peninsula. Gujarat has a population of around 60.4 million. It is the fifth largest state in India by area and ninth largest by population. The geographical features of Gujarat are influenced by climatic and tectonic forces prevalent on the Indian subcontinent. Kachchh Peninsula, Saurashtra Peninsula, and Mainland Gujarat are the major three physiographic regions in the area (Merh, 1995). Cenozoic, Precambrian and Mesozoic bedrocks are found in several locations of the state (Figure 2). Solid rock formations cover around 49% of the entire land of Gujarat while Quaternary Era deposits cover the rest of the region. The Cambay region, which is one of India's major proliferous basins, is located on the Indian plate's western boundary

and covers around 56,000 square kilometres. The Cambay region is an important section of the Mainland Gujarat geographical subdivision. The Saurashtra Peninsula is dominated by three major tectonic patterns: the Delhi trend (NE-SW), the Son-Narmada-Tapi (SONATA) trend (ENE-WSW), and the Dharwar trend (ENE-WSW and NNW-SSE).

Due to these physiographical trends, the Saurashtra Province is contained within a large horst which is primarily formed by Deccan trap motions which involves alkaline and basalt intrusions (Sharma, 2013). The Saurashtra Province is characterized by the Kim fault in the Saurashtra province shelf, peripheral faults accompanying the ESE-WNW trending Narmada rifting zone, as well as a NW-SE oriented minimal fault and the North Kathiwar fault which can be observed throughout the area.

In addition to the NW-SE structures, many significant patterns can be found, some of them oriented in N-S and E-W direction, indicating subsurface fault systems (Biswas, 1987). The important geothermal springs Tulsishyam and Savarkundla as well as the hot spring in Lalpur near the North Kathiawar fault are located along E-W and NE-SW lineaments. The Dholera geothermal spring is situated near the Saurashtra Peninsula border, crossing the West Coast boundary westwards of the Cambay Basin's West Margin fault. These geothermal springs are all located around high gravity anomalies, which indicate a thin mantle and the existence of granitic rock layers (Sharma, 2013).

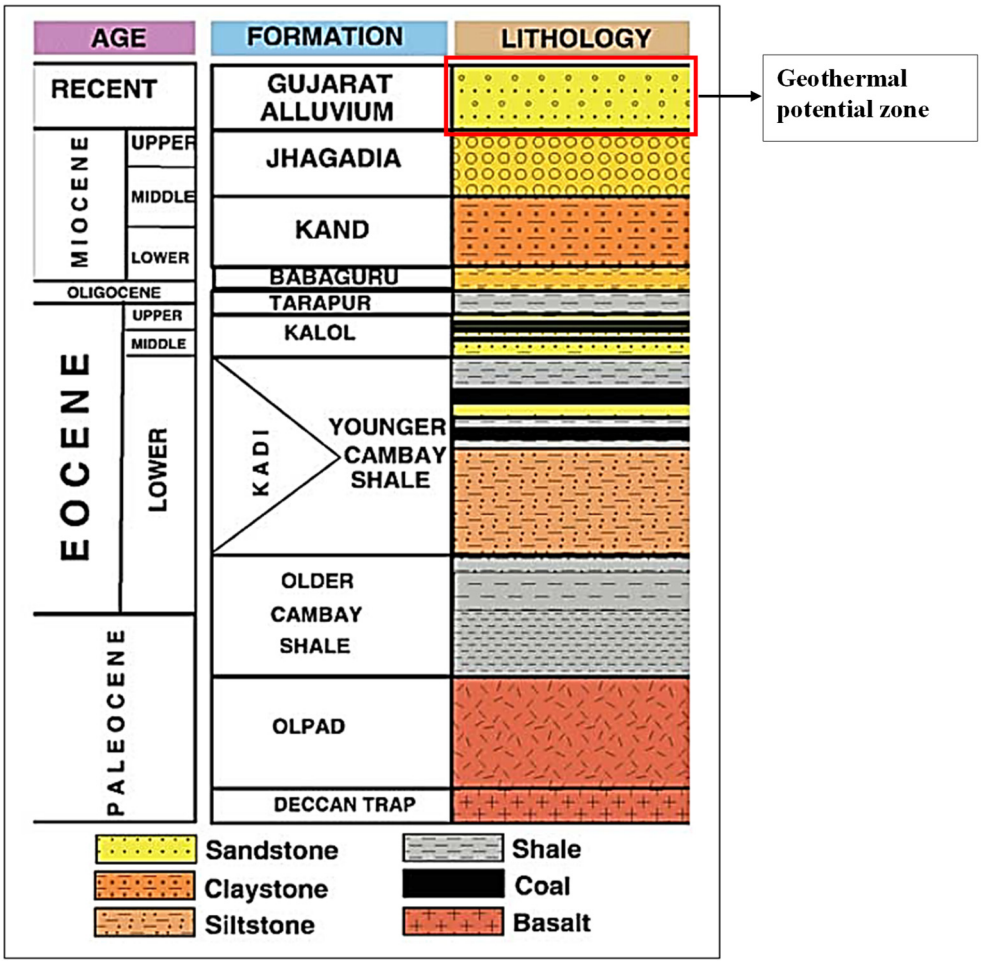


FIGURE 2: Sub-surface stratigraphy of Cambay basin (Singh et al., 2007)

The study area is near the Ahmedabad district of Gujarat. The Dholera geothermal zone lies between the Gulf of Khambhat's traditional port communities (Figure 3). It is located about 30 kilome south-west of Dhandhuka city in the Ahmedabad province. The territory is encompassed by ocean on 3 sides: in the north by Bavaliari Creek, in the south by Sonaria Creek, and in the east by the Gulf of Khambhat (Aghil

et al., 2014). The Saurashtra province is one of Gujarat's three primary physiographic subdivisions, located between 20° 30' N and 22° 30' N latitude and between 69°0' E and 72°30' E longitude. The Saurashtra peninsula seems to be the horst barrier between the crossing junction of Narmada, Kachchh and Cambay and is located along the western coast of the Indian peninsula (Biswas, 1987). The geographical height decreases in the Eastern part of the province. In western direction, the low ground rises by 8 meters whereas in the east it climbs by 4 meters. The landscape comprises wetlands, mud pools and salt plains.

The stratigraphy contains gravels, fine-grained to coarse-grained sand, and clay. The soil has a high salinity, is calcareous, and contains sandy loams as well as a substantial amount of montmorillonite (Yadav and Sircar, 2019). The sandstone, which seems to be the major rock in the subsurface, is divided into fine and coarse aggregate sand. The major hot springs in the Dholera region are situated in Bhadiyad, Utthan, and two in Swaminarayan temple at Dholera. The Dholera geothermal region in Gujarat has greatest flow rate of those four locations (Vaidya et al. 2015). The geothermal water in Dholera has a temperature range of 40-50°C with a flow rate of 4 l/s from each well. The water here is rich in sulphate, sodium, potassium, and chloride (Shah et al., 2017).

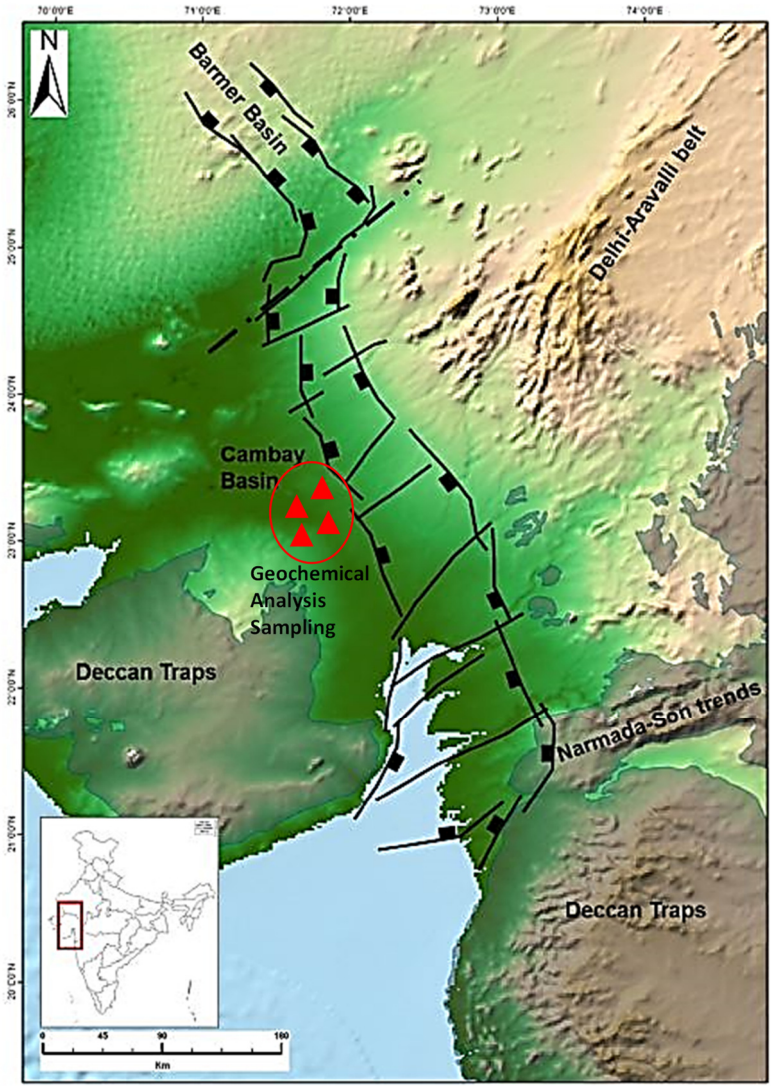


FIGURE 3: Tectonic framework of the Cambay basin. The figure encompasses the five major blocks of Cambay, namely Sanchar Patan block, Ahmedabad Mehsana block, Tarapur block, Broach block and Son-Narmada-Tapti block (Misra et al., 2019)

**2.2 Geochemistry**

In this section, physical and chemical parameters of geothermal water samples from different locations in Dholera are presented. Properties like salinity, hardness, colour, conductivity, cation and anion content, etc. were obtained from the literature. In Table 1, several chemical and physical parameters along with elemental composition of the geothermal water samples are listed. The salinity in Dholera geothermal water is observed to be moderate to high with salinity levels varying between 3000 and 4000 mg/l. Due to contact with granitic bedrock with high $Na^+$, $K^+$, and $Cl^-$ content, the groundwater has high salinity (Sharma, 2013). The salinity and total dissolved solids (TDS) are in accordance with the Dholera geothermal water. As chloride and sulfate are the main anion constituents in the samples, decreased carbonate hardness is expected. Sodium, potassium, chloride, and sulfate are some of the components found in geothermal waters. Carbonate and bicarbonate elements in low amounts suggest that the groundwater has ascended from greater depth. Boron is found in the water, indicating that it contains a mix of elements originating from Mesozoic strata. Fluoride is found in varying concentrations in all samples as shown in Table 1. High fluoride concentrations imply that all these waters were in contact with mica and apatite-bearing strata beneath the surface. The concentration of silicon (Si) in the geothermal water varies between 5 and 12 mg/l (Sharma 2013). Silicon influence is more probable at deeper levels when the temperature difference is larger. In silicon dioxide, alkali feldspar, and quartz, Si is dissolute. The pH of the thermal spring samples is between 6.5 and 7.4, reflecting changes in flow directions and temperature, as well as $CO_2$ depletion. Another possibility is that the waters have indeed been subjected to anthropogenic processes. The concentration of $SO_4$ varies from mild to high. The concentration of chloride in the research area is in-between moderate and high.

TABLE 1: Physical and chemical parameters of Dholera region (Yadav et al., 2021; Shah et al., 2021)

| Components/ Sample | Units (SI) | Utthan | Swaminarayan Temple | Bhadiyad | Dholera |
|---|---|---|---|---|---|
| pH | | 7.05 | 7.22 | 7.32 | 7.25 |
| Na | mg/L | 1140 | 1180 | 1160 | 1110 |
| K | mg/L | 26.5 | 25.7 | 21 | 23.7 |
| Ca | mg/L | 107 | 107 | 125 | 100 |
| Mg | mg/L | 49 | 50 | 72 | 46 |
| $SiO_2$ | mg/L | 12.3 | 16.9 | 9.98 | 12.8 |
| B | mg/L | 3.88 | 3.76 | 4.44 | 4.8 |
| Cl | mg/L | 2430 | 2510 | 2640 | 2480 |
| F | mg/L | 0.21 | 0.17 | 0.22 | 1.16 |
| $SO_4$ | mg/L | 30 | 13 | 56 | 16 |
| $HCO_3$ | mg/L | 190 | 160 | 140 | 170 |
| As | mg/L | 0.01 | 0.01 | 0.01 | 0.01 |
| Rb | mg/L | 0.002 | 0.002 | 0.002 | 0.002 |
| Cs | mg/L | 0.002 | 0.002 | 0.002 | 0.002 |
| Sr | mg/L | 0.002 | 0.002 | 0.002 | 0.002 |
| Ba | mg/L | 0.002 | 0.002 | 0.002 | 0.002 |
| Fe | mg/L | 0.505 | 0.482 | 0.01 | 0.647 |
| Mn | mg/L | 0.02 | 0.02 | 0.02 | 0.02 |
| Salinity | ppm | 3970 | 4040 | 4210 | 3940 |
| Conductivity | µmhos/cm | 6200 | 6400 | 6670 | 6190 |

The composition of the geothermal water is determined by the level of chloride. The ratio of anions and cations changes when conductance levels change. Water with a high salt and mineral content has superior ionic conductivity. The geothermal water samples in the area usually show meteoric characteristic as seen from key cation and anion measurements, indicating that meteoric water penetrates to great depth where it interacts with the bedrock, which has been heated by uplifted mantle. After reaching a temperature beyond the boiling point, the hot waters rises back to the surface as geothermal

waters. From the above analysis we can conclude that the geothermal waters found here are meteoric in nature.

### 2.3 Types of desalination processes

One of the oldest thermal desalination methods used to convert geothermal or saline water into potable drinking water is distillation. The concepts of heating, evaporation, and condensation are used. The water is boiled until it is fully evaporated. Then the vapour is cooled to make portable drinking water and the salt is left as residue. The necessary thermal energy is generally generated either from steam production, excess heat boilers, or by extracting back-pressure steam through turbines in geothermal power plants (Raluy et al., 2004). The most widely used thermal desalination techniques are Multiple Effect Distillation (MED), Multistage Distillation (MSF), Solar water desalination, Cogeneration, and Vapour Compression Evaporation (VC). Figure 4 presents the several types of desalination systems.

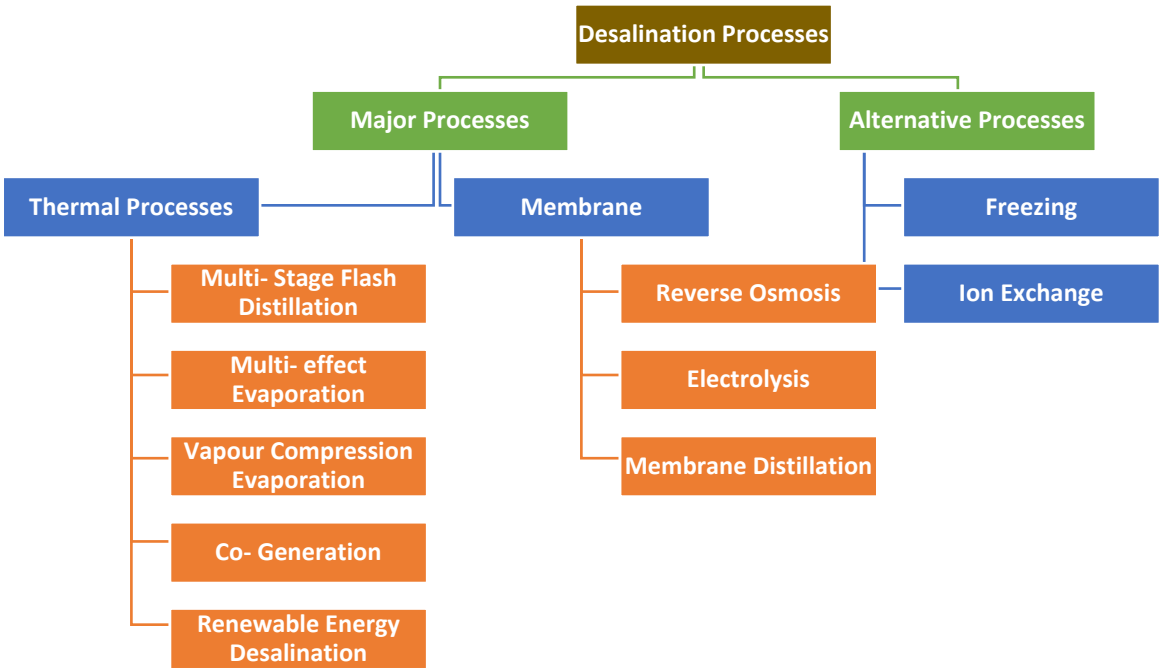


FIGURE 4: Types of desalination systems, including thermal, membrane and alternative processes (Shatat and Riffat, 2014)

#### 2.3.1 Thermal processes

***Multi-Stage Distillation System (MSF)***

For over a century, distillation of water in a vessel running at a lowered pressure has been employed to lower the boiling point of water (Figure 5). The MSF method was invented in the 1950s by the Scottish engineering firm Weirs of Cathcart, and it saw major development and extensive applications all through the 1960s owing to its economic scalability and capacity to perform on reduced steam (Hamed et al., 2001). Presently, MSF technology produces roughly 17.6% of the entire global freshwater supply. The Arab world is home to most MSF facilities. While the MSF procedure is most efficient for extracting fresh water from the sea, it is a high-energy procedure that necessitates both thermal and mechanical power (Hamed et al., 2001). In this study, it is assumed that the saline geothermal water is boiled in a brine heater container in the MSF distillation system until it reaches its boiling temperature. The geothermal water is boiled and then pushed through a series of containers in which the decrease in

pressure causes the geothermal water to evaporate or flash rapidly. The pressure inside the stage is the primary determinant of the amount produced (UN. ESCWA, 2001). The vapor is converted to freshwater by chilling in heat exchange tubes. The incoming geothermal water that flows to the brine heater keeps the pipes cold. By reducing the amount of heat needed in the brine heater chamber to raise the geothermal water temperature, thermal efficiency is enhanced.

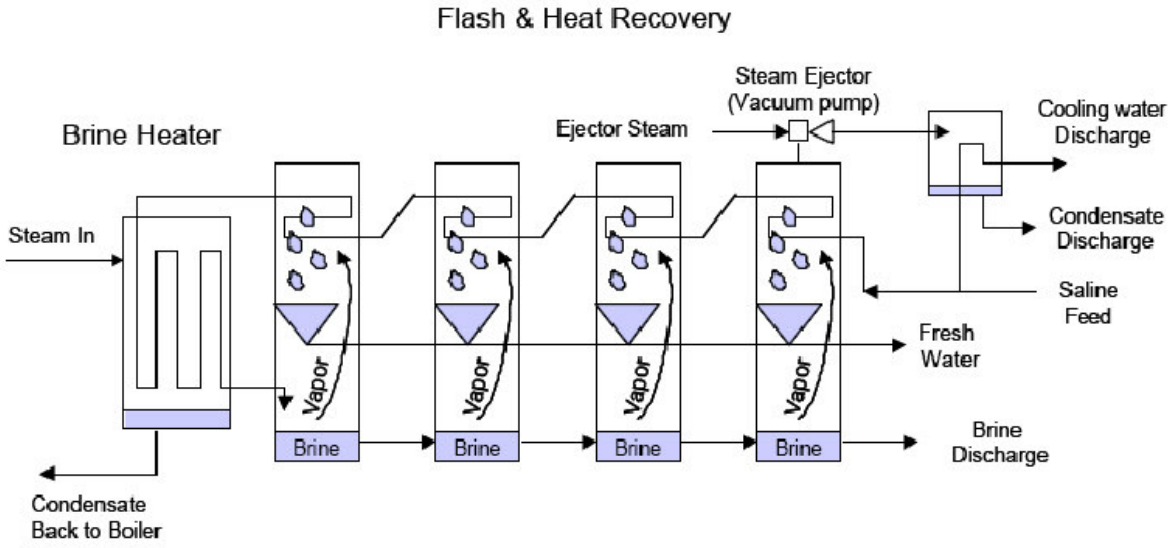


FIGURE 5: Basic schematic of Multi- Stage Desalination system (Eltawil et al., 2008)

***Multi-effect distillation (MED)***

For geothermal desalination, the MED procedure is the oldest large-scale distillation technology. MED plants currently provide 3.5 % of the globe's fresh water (Wangrick, 2000). Its most prominent feature is good quality of distilled water, high production capacity, and high energy performance (Al-Shammiri and Safar, 1999). MED has traditionally been utilized in the distillate manufacturing market for the vaporization of refined sugar, sugar cane juice and in the salt manufacturing process. The MED technique, like MSF, is carried out in a succession of containers or vaporization units, and it follows the very same vaporization and chilling concepts as MSF, that is by lowering working pressure in each stage of evaporation.

This approach permits the geothermal water input to boil multiple times without requiring additional heat after the initial contact. After being warmed in pipes, the geothermal water reaches the first unit and is heated to the boiling temperature. To enhance quick evaporation, the geothermal water is poured onto the exterior of the evaporator coils. Steam, typically from the dual power plant, heats the evaporator coils. The steam condenses on the opposite end of the tubing, and the steam condensate is reused as feed water for the boiler at the power station.

***Vapour-compression evaporation (VC)***

In addition to the vapor-compression distillation method, other procedures such as MED, described above, and vapor compression with single effect are also used. In this process, the energy for geothermal water vaporization comes from vapor - compression. In VC facilities, the pressure is reduced to lower the temperature of water. Two mechanisms, that is mechanical compression and steam jet technology, are used to cool the steam and to provide adequate heat to evaporate the incoming geothermal water.

Typically, the mechanical compression technique is powered by electricity or diesel. To increase the heat exchange and evaporation of geothermal water, VC devices have been designed in a range of

layouts. The compressor creates a vacuum in the evaporation chamber before compressing and condensing the steam extracted from inside the tube bundle. When geothermal water is poured on the outer layer of the warmed pipe bundle, it boils and then evaporates, releasing more steam.

A venturi aperture at the steam jet generates and gathers steam from vaporization, resulting in reduced ambient pressure in the VC distillation apparatus, also known as a thermo-compressor. The steam jet compresses the accumulated steam. This mixture cools on the pipe wall, supplying heat energy to evaporate the geothermal water within the vaporization chambers on both sides of the pipe walls.

### 2.3.2 Membrane distillation techniques

***Reverse osmosis (RO)***

In comparison to the previous techniques, the RO process is more recent, having been established as a viable method in desalination plants in the 1970s. By moving a membrane through a pressurised saline mixture, the water is separated from solvent components without the need for heat or phase separation. Most of the energy in this type of systems is required to increase the temperature and pressure of the feed water. An alternative description of the RO process is moving a solvent over a membrane surface at a pressure that is higher than the osmotic pressure between a higher and a lower concentration of solutes. Therefore, water flows through the membrane surface in the reverse direction of natural movement, accumulating dissolved salts in the process and raising the salt concentration (Ayyash et al., 1994). A typical large RO plant has four basic components: high pressure pumping, a RO membrane, a post-treatment strategy, and a pre-treatment mechanism (Khawaji et al., 2007). In recent times, the globes largest RO desalination facilities have been built in the Gulf Region, particularly Saudi Arabia.

***Electrodialysis Desalination Technique (ED)***

Electrolysis Desalination was first commercialized in the 1960s, almost ten years earlier than RO. It was a low-cost method to desalinate brackish water and it sparked a lot of attention in the development of desalination technologies for the production of fresh water for municipal usage (Buros, 2000). The method is also used in the chemical and ecological sectors, as well as in manufacturing of consumable salt (UN. ESCWA, 2001; Strathmann et al., 1992). ED is an electrochemical separation technology that makes use of electrostatically charged anion and cation exchanging membranes with electrostatic attraction as a main driver. Most ions in geothermal water are ionic, which means they are charged both anionic or cationic, and they gravitate toward conductors of opposite electrical charges. Membranes can be designed to allow cations or anions to flow through selectively.

***Membrane distillation (MD)***

Membrane Desalination was first studied in the 1960s, however, only few facilities were commercially operating in the 1980s (UN. ESCWA, 2001). This technology, which really is essentially a vaporization approach, is a membrane-based, high temperature heat driven process that combines distillation with membrane technology. It makes use of the difference in temperature between the supply solution that comes into touch with a micro-porous membrane on one end and on the other side of the membrane. This difference in temperature causes a change in vapour pressure, which causes the generated vapour to move across the membrane and into the condensing area. The entire process depends on the employment of hydrophobic membranes that are only permeable to vapour, avoiding liquid phase transition as well as the possible presence of dissolved particles (Mathioulakis et al., 2007). The vapour distils on a cooler surface after flowing through the membrane, producing fresh water. Because clean water cannot cross the membrane, it must be retrieved as a freshwater discharge (Buros, 2000). Even though MD initially did not have much industrial success, current research and development have proven that small scale MD distillation technology work reliably with solar energy and might have potential for future usages.

### 2.3.3 Alternative processes

***Freezing***

During the 1950s and 1960s, extensive trade research was conducted to increase the efficiency of the freezing technique. The fundamentals of freezing distillation are straightforward. Disintegrated salts are excluded from the production of ice crystals during in the recrystallization process. Under regulated conditions, geothermal water can become desalinated water by chilling it to produce crystals. Before the full volume of water is frozen, it is normally cleaned and washed to eliminate salt that may remain in the leftover water or adhere to the ice crystals. After that, the ice is melted to provide fresh water (Buros, 2000). Cooling and melting, the two principles of heat transfer, are both regenerating, leading to extraordinarily high energy efficiency (Rice and Chau, 1997). Over the last 40 years, a modest number of facilities have been erected, but the technique has not been commercially successful in the provision of freshwater resources for municipal use. A solar-powered prototype unit built in Saudi Arabia in the late 1980s is perhaps the most recent important example of desalinating by chilling, but that facility has since been dismantled. The freezing technique is probably best suited for the removal of toxic waste rather than for the provision of potable water (Buros, 2000).

***Ion exchange***

Ion interchange membranes have evolved from a scientific tool to an engineering material with important technological and commercial implications in the last half - century. Ion exchange membranes are garnering a lot of attention these days, and they are being used to desalinate sea and brackish water, as well as clean wastewaters. They are useful for focusing or isolating ionic components contained in food products and medicines, as well as for making basic industrial chemicals (Xu, 2005). Ion convertors are inorganic or organic compounds which can swap one type of isolated ion in a solvent for a different type of ion. A cation converter, for example, can replace Na ions in an aqueous solution with H, and an anion exchanger can then replace $Cl_2$ with $OH_2$, resulting in the complete 'demineralization' of a NaCl solution. By utilizing an acid to rejuvenate the cation converters and a base to rejuvenate the anion converter, the operation could be inverted. Ion convertors are a feasible way for completely decalcify water in high-purity utilizations such as high-pressure furnaces. Unfortunately, due to its high cost, it is not suited for purifying and desalinate water or geothermal water (Miller, 2003). Table 2 represents the advantages and disadvantages of different desalination systems.

## 2.4 Selection of source and desalination system

Solar receivers are a type of heat exchangers that transform reflected, refracted, and radiant solar ray energy into heat or electrical energy which is then stored in a transmission medium. The most critical component of any solar receiver is the solar thermal receiver. This is a piece of technology that captures solar energy and converts it into heat and then transfers that collected heat into a fluid. Static receivers and concentrating receivers are two types of solar receivers (Figure 6). A static receiver detects and absorbs solar energy in one spot, whereas a sun-tracking focused solar power receiver captures and concentrates the sun's radiation from a wider collection area, increasing the radiation intensity.

Table 2 provides an overview of several types of collectors presently available. FPC, ETC, and focusing collectors are examples of this.

TABLE 2: Pros and Cons of key desalination techniques used worldwide

| Desalination system | Pros | Cons |
|---|---|---|
| Reverse Osmosis | • Low CAPEX<br>• Fast start-up with simple operation<br>• High production capacity with 30-60% of recovery efficiency<br>• Removes other contaminants together with the salt | • Higher chemical and membrane maintenance costs<br>• Unable to adapt to changes in water quality<br>• Adequate pre-treatment is required |
| Multi-stage flashing (MSF) (Brogioli et al., 2018; Mabrouk and Fath, 2015) | • Designs with a large capacity<br>• Technology that has been proven to be reliable and has a long operational life<br>• Scaling is less likely while flashing rather than boiling. Feed water only needs to be pre-treated to a minimum.<br>• The cost and procedure of the plant are unaffected by salinity levels.<br>• Thermal energy can be obtained by combining electricity generating with heat energy production. | • A significant financial investment is required.<br>• Process consumes a lot of energy which leads to large footprint<br>• Corrosion issues if low-quality materials are employed<br>• Slow start-up (hours)<br>• Plants are frequently shut down for maintenance. High-level technical expertise is necessary. |
| Multi-effect desalination (MED) (El-Sayed and Silver, 1980) | • Feed water only needs to be pre-treated to a minimum. Process is very reliable, and it only requires a small number of people to run it. It can handle standard amounts of suspended and organic debris.<br>• Thermal energy can be obtained by combining electricity generating with thermal energy production.<br>• Water of exceptional quality | • Excessive energy use<br>• High start-up and operating costs<br>• High-quality materials are essential because the procedure is corrosive.<br>• Before being used as potable water, product water must be cooled and blended. |
| Electro-dialysis reversal (EDR) (Chehayeh and Lienhard, 2017) | • The amount of energy used is proportional to the amount of salt removed rather than the volume treated.<br>• A membrane with a lifespan of 7–10 years. Low to moderate pressure performance | • Only appropriate for feed water with a TDS of up to 12,000 mg/L. Membrane cleaning is necessary on a regular basis.<br>• Membrane stacks may experience leaks.<br>• Bacterial pollutants are not eliminated by the system, necessitating post-treatment for potable water. |

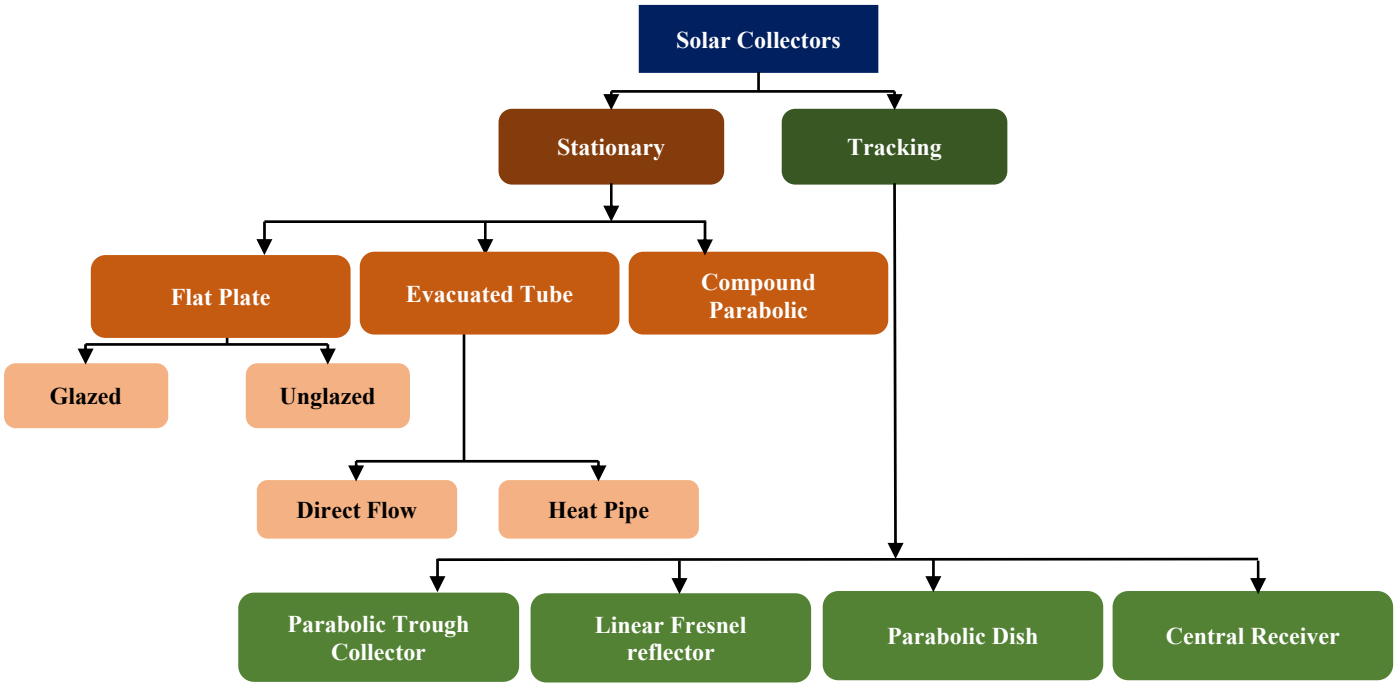


FIGURE 6: Classification of solar collectors (Kalogirou, 2004)

TABLE 3: Solar energy collectors (Kalogirou, 2004)

| Motion | Collector Type | Absorber Type | Energy Concentration Ratio | Indicative Temperature range (°C) |
|---|---|---|---|---|
| Stationary | Flat Plate Collector (FPC) | Flat | 1 | 30-80 |
| | Evacuated Tube Collector (ETC) | Flat | 1 | 50-200 |
| | Compound parabolic Collector (CPC) | Tubular | 1-5 | 60-240 |
| Single- axis tracking | | | 5-15 | 60-300 |
| | Linear Fresnel Reflector (LFR) | Tubular | 10-40 | 60-250 |
| | Parabolic Trough Collector (PTC) | Tubular | 15-45 | 60-300 |
| | Cylindrical Trough Collector (CTC) | Tubular | 10-50 | 60-300 |
| Two- axis tracking | Parabolic Dish Reflector (PDR) | Point | 100-1000 | 100-500 |
| | Heliostat Field Collector (HFC) | Point | 100-1500 | 150-2000 |

### 2.4.1 Static collectors

Important distinctions of solar collectors are the movement of the solar panels, as well as the operating temperature. Solar thermal receivers that are static are fixed in one location and therefore do not rotate with the solar radiation. There are three types of receivers in this category namely Evacuated Tube Collectors (ETC), Stationary Compound Parabolic Collectors (CPC) and Flat Plate Collectors (FPC).

***Flat plate collectors (FPC)***

When sunlight reaches a black absorption area with strong absorption properties via a transparent glass, a significant part of the heat is collected by the panels and delivered through the transmission media in the fluid pipes where it is stored or used. The base of the absorber tube along with the enclosing edge are suitably insulated to avoid transmission heat losses. The liquid tubes could be attached to the absorbing panel or moulded into the panel. On both ends, large diameter header tubes connect the fluid tubes. The opaque cap is used to prevent convective loss from the absorber area by restricting the static air column between both the absorber surface and the glass. The glass is opaque to short wavelength solar irradiance but nearly transparent to long wavelength thermal heat radiation that is emitted by the absorber area, reducing collector radiation heat losses.

***Static compound parabolic collectors (CPC)***

CPCs are receivers which have no need for scanning. They can redirect all incoming solar radiation towards absorbers within specific restrictions. Winston (1974) emphasized their possibilities as solar thermal collectors. Using a trough with two parts of a parabola opposite each other can eliminate the need to move the collector to accommodate changing solar direction. Compound parabolic projectors can absorb irradiation from a wide range of directions. Because of the repetition applied and included, any irradiation hitting the apertures within the receiver acceptance angle finds its way to the absorber surface at the base of the receiver.

***Evacuated tube collectors (ETC)***

Flat rate solar thermal receivers were created with the intention of being used in sunny, warm climates. Their benefits are significantly reduced when weather conditions are unfavourable, including cold, gloomy, and stormy days. Moreover, environmental impacts such as condensate and humidity will cause internal components to deteriorate sooner than expected, resulting in system failure. Solar thermal receivers (tubes) with evacuation heat pipes function differently from regular receivers (Figure 7). In such solar thermal receivers, a constant heat tube is encased within a pneumatically sealed tube. It has been demonstrated that a well-chosen surface paired with efficient convective control can produce outstanding results at high temperatures (ASHRAE, 1995). The collector can work at higher degrees than FPC because the vacuum environment decreases convective and propagation losses. They gather reflected and transmitted radiation, just like FPC. At low incident angle, however, they are more efficient. In terms of day-to-day efficiency, ETC should be favoured over FPC.

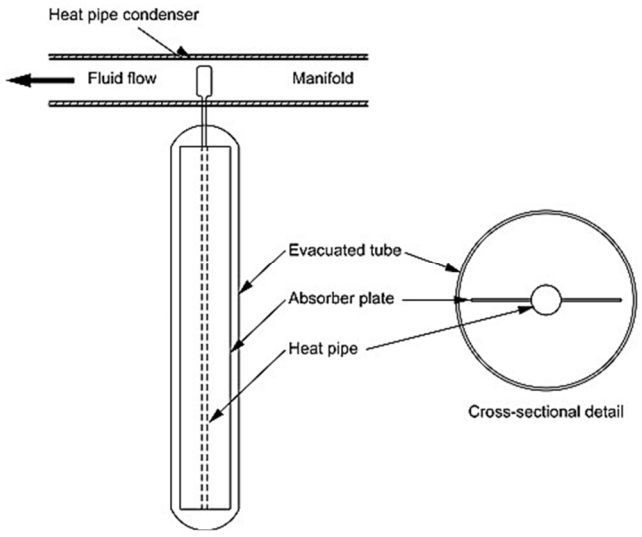


FIGURE 7: Components of evacuated tube collectors (Zhang and Yang, 2019)

### 2.4.2 Sun tracking concentrating collectors

By minimizing the surface area through which heat loss occurs, the temperature of the heat delivery mechanism can be increased. Temperatures beyond those attained by FPC can be attained if a large amount of solar irradiance is focused on a small receiver location. This is achieved by putting an optical device between the solar irradiation source and the heat absorbing area. Focused thermal receivers have few benefits over flat-plate thermal receivers (Kalogirou et al., 1994). The receivers which fall in this category are Linear Fresnel Reflectors, Parabolic Dishes, Central receivers, and Parabolic Trough collectors.

## 3. METHODS

### 3.1 Designing of an MSF system with an evacuated tube collector

### 3.1.1 Thermodynamic analysis of an evacuated tube collector

The following equations are used for mathematical modelling of the evacuated tube collector which is used in this study. The quantity of heat absorbed by the evacuated tube collector is calculated as shown in Equation 1:

$$Q_{absorber} = A_{collector} \times l_{intensity} \times n_{optical} \quad (1)$$

Where $Q_{absorber}$ is the absorbed heat (W), $A_{collector}$ is the area of the collector ($m^3$), $l_{intensity}$ is the intensity of solar radiation ($W/m^2$) and $n_{optical}$ is the optical efficiency. The total area exposed to collector is given by Equation 2:

$$A_{collector} = \pi \times d \times l \times n \quad (2)$$

Where d is the diameter of evacuated tube (mm), l is the length of evacuated tube (mm) and n is the number of evacuated tubes.

The heat loss to the surrounding by the solar collector is given as (see also equation (5)):

$$Q_{loss} = A_{collector} \times F_{heat\ loss} \times (S_{collector} - U_{Loss}\,(T_{inner} - T_{average})) \quad (3)$$

Where $Q_{loss}$ is the heat loss (W), $F_{heat\ loss}$ is the heat loss factor, $S_{collector}$ is the solar energy falling on the collector ($W/m^2$), $U_{Loss}$ is the heat loss coefficient, $T_{inner}$ is the inner temperature of the evacuated tube and $T_{average}$ is the average temperature of the evacuated tube.

The net heat gain by the collector is given as:

$$Q_{useful} = Q_{absorbed} - Q_{loss} \quad (4)$$

Where $Q_{useful}$ is the useful heat (W).

The heat absorbed by the ETC is given as:

$$H_{absorbed} = Q_{absorbed} + Q_{useful} = \left(A_{collector} \times l_{intensity} \times n_{optical}\right) + A_{collector} \times F_{heat\ loss} \times (S_{collector} - U_{Loss}\left(T_{inner} - T_{average}\right)) \quad (5)$$

Where $H_{absorbed}$ is the heat absorbed by the evacuated tube (kJ), $\Delta T$ is the temperature difference at each stage (°C), $T_{flash}$ is the temperature of the flash (°C), and $T_{brine}$ is the temperature of the brine (°C).

### 3.1.2 Thermodynamic analysis of an MSF system

The aims of this part of the study are:

1. To develop a thermodynamic model for solar evacuated tubes system according to the need of Multi-Stage Distillation system;
2. To develop a thermodynamic model for the Multi- Stage Distillation system for geothermal water desalination;
3. To simulate the production of heat from an evacuated tube solar collector with the geothermal Multi-Stage Distillation system to separate steam and salt; and
4. To estimate the performance characteristics of the system, including total mass and salt balances, heat transfer unit rate equations, and energy balances for the brine heater.

A Python program was made for developing and computing the thermodynamic model of the solar and MSF distillation systems. The simulation was done based on the overall heat and mass transfer coefficients, salt mass balance, pressure, and temperature as well as with the rate of evaporation. The input parameters which were used are taken from geochemical and geophysical studies which were performed on the geothermal resources of Dholera, Gujarat, India, as discussed in section 2. The Dholera geothermal field contains a huge resource of low enthalpy geothermal energy. There is a shortage of drinking water in the region and desalination of the geothermal water can produce potable drinking water. The parameters like mass flowrate, temperature, salt concentration, etc. are taken from the physio-chemical analysis of geothermal well data from Dholera (Shah et al., 2017).

Table 4 shows the input parameters which were used for designing the model of the Solar-MSF geothermal desalination system:

TABLE 4: Design parameters used for the Solar MSF geothermal desalination system

| **Parameters** | **Values** |
|---|---|
| Geothermal water temperature from well | 40°C |
| Geothermal water mass flowrate from well | 7 l/s |
| Separation temperature | 150°C |
| Pressure conditions | 1-7 bar (all pressure and heat losses are considered negligible) |
| Inlet temperature of solar evacuated tubes | 40°C |
| Salinity of geothermal water | 3940 – 4210 ppm |
| Specific heat for all liquid streams | Constant for each |
| Effect of non- condensable gases on the heat transfer process | Negligible |
| Salt Concentration of distilled water | Less than 1000 ppm (freshwater condition) |

A process diagram of the solar MSF geothermal desalination system is shown in Figure 8. The major components of the geothermal desalination system include a brine heater, a flashing container which comprises the pre-heater tubes, a brine pool and a distilled water tank. The MSF system modelled here is a three-stage system. The number of stages was decided based on the water temperature when it

converts from steam to water. The source of water is a geothermal well in Dholera.

The feed water comes from a geothermal well with a temperature of 40°C, a flowrate of 7 l/s and 1 bar pressure (Point 1 in Figure 8). It is then pumped into the MSF chambers with 7 bar inlet pressure (Point 2) passing through the other two MSF chambers (Point 3 & 4). The heat transfer in the brine heater raises the temperature of the feed saltwater to the highest saline temperature at stage 1 (Points 3 & 4). The water is then pushed into the solar evacuated tube at a temperature of 91.4°C and a pressure of 6.4 bar (Points 5 & 6). With 5.9 bar pressure, the geothermal water is heated to 150°C (Point 7). At 143°C and 4 bar pressure, the hot brine reaches the flash phase (Point 8). The pressure here is lower than that of the brine's saturation point. This permits the stream to flow freely throughout the device without using pumping force. Heat is delivered to the geothermal water by condensation of a small quantity of the brine within the evaporator while the brine passes through the flash compartment. The produced vapour passes an item of equipment that prevents contamination of the product with brine droplets trapped in the flash-off vapor. As the vapour condenses in the thermal water condenser/preheater pipes at Point 4, its temperature decreases. The condensed vapor is gathered in the distillation tray (Point w1), resulting in high quality distillate water, which subsequently exits the unit at Point w2 at Stage 2. It then passes Point 9 and enters Stage 2. The salt concentration of distilled water at Stage 1 is estimated to be 142 ppm with mass flow of 0.09 kg/s. The same process is continued at Stage 2 where the brine water enters with a temperature of 116.9°C and 1.8 bar pressure (Points 9 &10). The amount of distilled water produced at Stage 2 is 0.45 kg/s with a salt concentration of 164 ppm (Point w2). This water leaves Stage 2 and enters Stage 3 at a temperature of 99.6°C with 1 bar pressure (Point 11 & 12). The amount of distilled water produced in this stage is 0.66 kg/s with a salt concentration of 194 ppm (Point w3). The rejected water from the system can be further used for direct applications like food drying, milk pasteurization, etc. where salinity is not an issue (Point 13).

The following is a basic thermodynamic version for the Geothermal Multi-Stage Flash Distillation (MSF) procedure, which will serve as a first step toward a more complete mathematical model that will be constructed when more precise information will become available in the future.

The temperature difference at each stage can be calculated by:

$$\Delta T = \frac{T_{flash} - T_{brine}}{n} \tag{6}$$

Where n is the number of stages, $T_{flash}$ is the temperature of the flash (feed water) and $T_{brine}$ is the temperature of the brine at that stage.

By using Equation (6) we can calculate the outlet temperature at each stage as follows:

$$T_1 = T_{brine} - \Delta T$$

$$T_{j+1} = T_j - \Delta T \tag{7}$$

Where $T_1$ is Temperature at stage 1 (°C) and $T_{j+1}$ is the temperature at stage j+1 (°C)

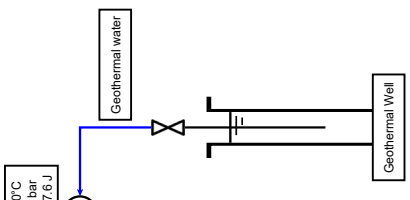

The mass flowrate of distilled water at every stage is estimated using the equation below:

$$\dot{m}_{distilled} = l_{heat} \cdot \dot{m}_{recoverable} \cdot (1 - l_{heat})^{j-1} \quad (8)$$

Where $\dot{m}_{recoverable}$ is the recoverable brine water that comes back to the MSF unit, and the $l_{heat}$ parameter is the amount of specific latent heat, which can be obtained with the equation:

$$l_{heat} = \frac{C_p \times \Delta T}{\lambda_{average}} \quad (9)$$

Where $C_p$ is the specific heat and $\lambda_{average}$ can be calculated with the equation (Gao et al., 2020):

$$\lambda_{average} = \left(0.00158927 \times (T^2)\right) - (2.36418 \times T) + 2500.7 \quad (10)$$

The total mass and salt balance equation is:

$$\dot{X}_{distilled} = \frac{\left((x_{flash} - x_{brine}) \times \dot{m}_{flash}\right) + (x_{brine} \times \dot{m}_{distilled})}{\dot{m}_{distilled}} \quad (11)$$

Where
$\dot{m}$ = mass flow rate;
$\dot{X}$ = salt concentration;
$x$ = mass fraction;
brine = brine stage;
flash = flash stage; and
distilled = distilled stage.

The required mass flow rate of the steam $\dot{m}_{distilled}$ is obtained as follows:

$$\dot{m}_{distilled} = \frac{\dot{m}_{recoverable} \times C_p \times (T_{brine} - T_{distilled,1})}{\lambda_{average}} \quad (12)$$

Where $\dot{m}_{recoverable}$ is the mass of recoverable brine water (kg/sec) and $C_p$ is the specific heat of water (J/kg°C).

The performance ratio of desalination units is very important for comparing different technologies and it is defined as follows:

$$Performance\ Ratio = \frac{\dot{m}_{distilled}}{\dot{m}_{steam}} \quad (13)$$

The next equation is used to calculate the mass flow rate of desalinated water:

$$\dot{m}_{flash} = (\dot{m}_{brine} + \dot{m}_{distilled}) \quad (14)$$

where $\dot{m}_{flash}$ is the mass flow rate of the supplied geothermal water, $\dot{m}_{brine}$ is the mass flow rate of

the brine discharge and $\dot{m}_{distilled}$ is the mass flow rate of the desalinated water at each stage. The mass flow rate of brine discharge is then calculated by:

$$\dot{X}_{flash}\dot{m}_{flash} = \dot{X}_{brine}\dot{m}_{brine} \quad (15)$$

where $\dot{X}_{flash}$ is the water salinity of the source and $\dot{X}_{brine}$ is the salinity of the brine. The heat transfer at each stage is obtained as follows:

$$\dot{Q} = \dot{m}_{steam}\,(h_j - h_{j+1}) \quad (16)$$

where j is the number of the stage, where the heat transfer is taking place from the distilled water to the geothermal water.

### 3.2 Material selection and corrosion protection

The composition of scaling-material in geothermal systems is frequently complicated, and it is influenced by a number of factors, including the geothermal water temperature and pressure, water-rock interactions, and the operational circumstances. Scale composed of calcium carbonate is commonly seen in systems with low - medium temperature brines (T<150°C) (Owen and Michels, 1984; Coris, 1986). Because thermal fluids contain dissolved $CO_2$, $H_2S$, $NH_3$, and chloride, which can lead to corrosion of metallic components, the materials used in geothermal facilities must be carefully chosen. Because of its complex design, thermal desalination involves a variety of corrosive processes. Uniform corrosion, pitting corrosion, crack corrosion, strass damage process, sulphur stress corrosion busting, hydrogen bubbles, intergranular corrosion, and galvanic corrosion are the most common corrosion types found in such facilities. Fatigue corrosion and alloy composition disintegration also occur. Corrosion problems arise at several stages of the Multistage Distillation desalination process. Table 5 lists the corrosion rates of metals at different velocities at ambient temperature (Arshad, 1986).

TABLE 5: Typical corrosion rates of metals in geothermal water moving at different velocities (Arshad, 1986)

| Material | Typical corrosion rates (mg/dm$^2$/day) | |
|---|---|---|
| | Velocity = 0.3 m/s | Velocity = 8.2 m/s |
| Carbon steel | 34 | 254 |
| Cast iron | 45 | 270 |
| Silicon bronze | 1 | 343 |
| Admiralty brass | 2 | 170 |
| Aluminium bronze (10% Al) | 5 | 236 |
| Aluminium brass | 2 | 105 |
| 90/10 Cu-Ni (0.80% Fe) | 5 | 99 |
| 70/30 Cu-Ni (0.05% Fe) | 2 | 199 |
| 70/30 Cu-Ni (0.50% Fe) | 1 | 39 |
| Monel | 1 | 4 |
| Stainless steel (type 316) | 1 | 1 |
| Titanium | 0 | 0 |

The corrosion at different stages of the desalination system is described in the following sections.

### 3.2.1 Vapour corrosion

MSF desalination facilities have less well-controlled vapor space circumstances, and considerable corrosion has been observed at rates exceeding the specified corrosion limit both, in acid and chemical dispensing vessels. In addition to the steam that is usually present, non-condensable gasses produced by the brine chamber are noted. The most frequent gasses are $O_2$, $N_2$ and $CO_2$. Stainless steels are nearly impervious to condensates formed by water, $CO_2$ and air combinations.

### 3.2.2 Corrosion in flash chambers

Carbon steel is the most common building material for flash chambers. They are used as a coating along with stainless steel or Cu-Ni in the early or all processes. Epoxy coating can be used for the same reason. Flash tanks are prone to extreme corrosion which can lead to metal breakdown. The function of oxygen in the MSF distillation facilities' various equipment, especially in the evaporators, is very complicated.

### 3.2.3 Heat exchangers

The single most significant component in an MSF facility is tubing for the heat exchanger. Heat exchange pipes are responsible for more than over 70% of corrosion problems in desalination facilities, which is reasonable (Coris, 1986). Geothermal water and cooling vapours, which have radically different characteristics, are running through tubing in heat exchangers. These liquids expose the tube to extreme environments in terms of corrosion.

### 3.2.4 Brine heater

Because these scales are generally very hard and difficult to eliminate using chemical methods, manual cleansing is employed in some circumstances. The brine furnace (which are part of evaporation chamber) is the warmest component of the exchanger with a powerfully scale producing fluid, therefore, in many of those facilities, 70/30 Cu-Ni or improved 66/30/2/2 Cu-Ni-Fe-Mn alloy is employed as the brine heating tube material.

### 3.2.5 Distillate system

Due to the breakdown of non-condensable carbon dioxide as well as other gasses, the distillation process must manage brine rich fluids.

### 3.2.6 Venting system

The venting system is a part of the equipment in which non-condensable gases (in case if we use it in future) can be handled. It is made up of a series of tubes that run from the heat exchanger to the flash tanks, either venting immediately or streaming down compartments before venting. After passing through the ejector capacitors, the expelled gases are directed to ejectors (in case if we use it in future). When describing ejection capacitors, three terminologies are used: "vent condensation", "inner condensation", and "post condensation".

## 4. MSF SYSTEM COST ANALYSIS

The cost for all components, pumps, valves, and actuators for the evaporator are estimated in detail below. Electricity and energy steam prices are assessed and computed on basis of Abdul and Mabrouk (2010).

The entire MSF price is calculated assuming a 20-year plant life cycle. As a result, the final water price is determined. Each element in the desalination plant's yearly investment cost is determined using the following formula (Abdul and Mabrouk, 2010):

$$Annual\ investment = CAPEX \times \frac{i \times (1+i)^{n1}}{(1+i)^{n1}-1} \tag{17}$$

Where CAPEX is the capital expenditure ($), $i$ is the interest rate (%) and $n1$ is the plant life-time.

The service and maintenance expenses are determined by multiplying the instrument acquisition cost of a component with the equipment index using an interest rate of i = 7% and an amortization time of n1 = 20 years. The distillation plant's hourly cost ($/h) is determined as follows:

$$hourly + CAPEX = \frac{Total\ annual\ investment}{365 \times 24 \times 60} \tag{18}$$

Similarly, the hourly OPEX is calculated as follows:

$$hourly + OPEX = LP\ steam + Electricity \tag{19}$$

Where OPEX is Operational expenditure (US$), and LP Steam is low pressure steam (bar).

Then, the unit product cost of the desalinated water (US$/m$^3$) is calculated as follows:

$$Unit\ Product\ cost = \frac{hourly\_CAPEX + hourly\_OPEX}{hourly\_Product} \tag{20}$$

Where $hourly\_CAPEX$ is CAPEX for one hour, $hourly\_OPEX$ is OPEX for one hour and $hourly\_Product$ is product cost for one hour.

## 5. RESULTS AND DISCUSSION

### 5.1 Multi-stage flash distillation system

As model input, the temperature of the water and the salt content are set to 40°C and 4210 ppm, respectively. The temperature at the first brine stage inlet is 143.5°C (Point 8 in Fig 8), the flow rate of the geothermal input water is 7 kg/sec, the rejected brine mass flow rate after the desalination process is 6.34 kg/sec, and the distillation water flow rate is 0.66 kg/sec. A steady-state model of the thermal water desalination process is provided using the pertinent variables and operational parameters. Table 6 displays the simulation findings. The streaming mass flow rate, distillation mass flow rate, temperature field of each flash cell, brine content, and steam usage can all be calculated using this method. In particular, the brine evaporation rate and steam generation temperature at each step are calculated.

More simulations were run to examine the impacts of the temperature of the geothermal feed water, the vapour temperature, and the saltwater temperature, as well as high - salinity and distilled water mass flow rate on the performance of the steady-state prototype of the MSF desalination process. Only the analysed variable was altered and all other variables were kept constant while the model estimated the performance of the system and the values of state variables.

The temperature of the geothermal input water, which changes with time, is an essential variable in the MSF desalination process. It affects the mass water flow rate of the fluid. The temperature variation of

the geothermal water was modelled to be between 40°C and 143°C, and the findings are given in Figure 8. The mass flow rate of the geothermal water declines with decreasing temperature at each step, as seen in the diagram.

TABLE 6: Simulation results of solar MSF geothermal desalination system (see Figure 8)

| Fluid Type | Step No. | Temperature (°C) | Pressure (bar) | Enthalpy (kJ/kg) | Mass (kg/s) | Quality of Steam | Salt Concentration (ppm) |
|---|---|---|---|---|---|---|---|
| Geothermal | 1 | 40 | 1.0 | 167.6 | 7.0 | - | 4205 |
| Geothermal | 2 | 40.1 | 7.0 | 168.5 | 7.0 | - | 4205 |
| Geothermal | 3 | 57.6 | 6.8 | 241.7 | 7.0 | - | 4205 |
| Geothermal | 4 | 84.5 | 6.6 | 355.7 | 7.0 | - | 4205 |
| Geothermal | 5 | 91.4 | 6.4 | 383.3 | 7.0 | - | 4205 |
| Geothermal | 6 | 91.4 | 6.4 | 383.3 | 7.0 | - | 4205 |
| Geothermal | 7 | 150.0 | 5.9 | 632.2 | 7.0 | - | 4205 |
| Geothermal | 8 | 143.5 | 4.0 | 632.2 | 7.0 | 0.0129 | 4205 |
| Geothermal + Heated Brine | 9 | 143.5 | 4.0 | 604.7 | 6.91 | 0.0 | 4347 |
| Geothermal + Heated Brine | 10 | 116.9 | 1.8 | 604.7 | 6.91 | 0.0515 | 4905 |
| Geothermal + Heated Brine | 11 | 116.9 | 1.8 | 490.7 | 6.55 | 0.0 | 5069 |
| Geothermal + Heated Brine | 12 | 99.6 | 1.0 | 490.7 | 6.55 | 0.0324 | 5886 |
| Geothermal + Heated Brine | 13 | 99.6 | 1.0 | 417.5 | 6.34 | 0.0 | 6080 |
| Distilled Water | w1 | 143.6 | - | 604.65 | 0.09 | - | 142 |
| Distilled Water | w2 | 116.9 | - | 490.7 | 0.45 | - | 164 |
| Distilled Water | w3 | 99.60 | - | 417.5 | 0.66 | - | 194 |

As seen in Figure 9, the mass flow rate of the geothermal water is sensitive to the change of geothermal water temperature, while the mass flowrate is nearly unaltered. Whenever the number of flash chamber levels remains constant, the temperature difference between the stages should be lowered for the entire process. This situation will directly affect the distilled water production, as shown in Figure 10. As the temperature of the geothermal water increases, the distilled water production decreases significantly. The temperature of vapourised fluid and geothermal water will be the same in the flash chamber. Due to high temperature the water vapour will have low density and will not get much time to condense and settle down as water. Hence, there will be less distilled water produced if the temperature of the geothermal water is high. In Figures 9, 11 and 12, S1, S2 and S3 represent the stages of flash chambers, whereas i and o represent the inlet and outlet of the relevant stage.

Figure 11 shows the relation between temperature and pressure. It has been observed that the pressure drop at each stage also leads to a drop in temperature at each stage

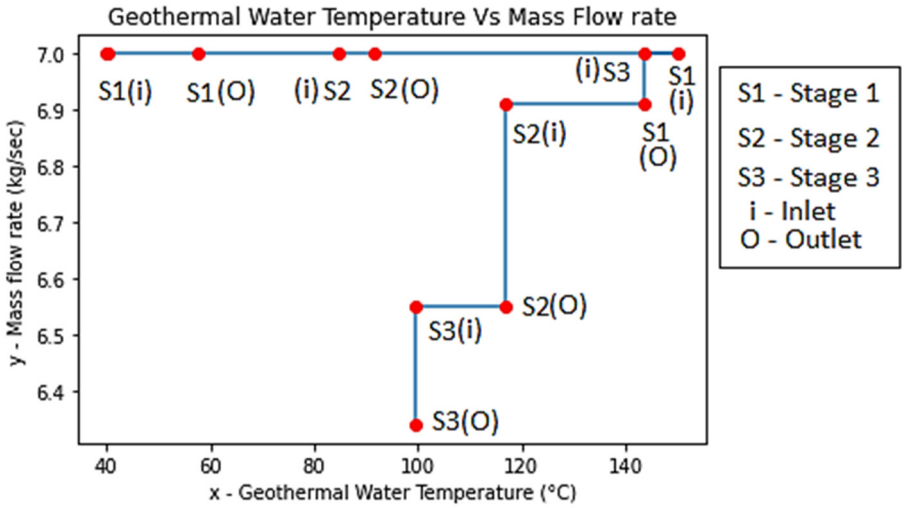


FIGURE 9: Geothermal water temperature vs mass flow rate

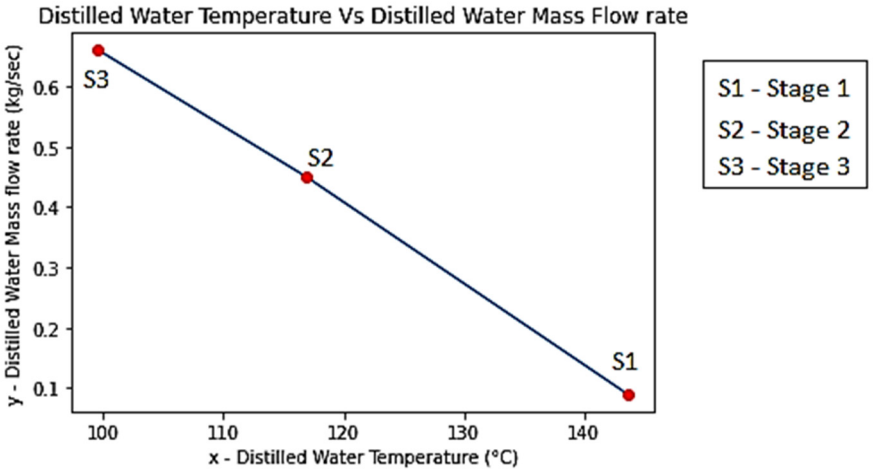


FIGURE 10: Distilled water temperature vs distilled water mass flow-rate

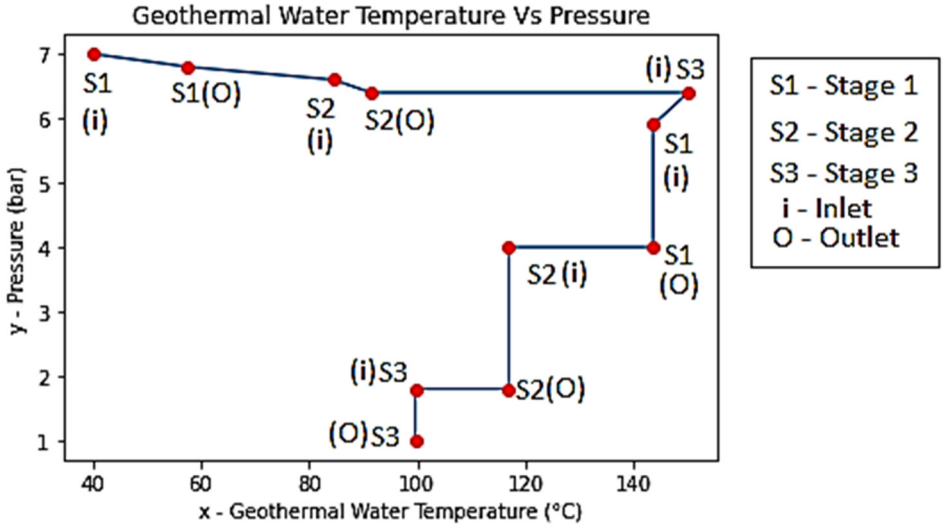


FIGURE 11: Geothermal water temperature vs pressure

It can be observed in Figure 12 that the salt concentration in the brine increases with decreasing brine temperature at each stage. Hence, the salt concentration at Stage 1 for a brine temperature of 143.5°C is around 4350 ppm. Similarly at Stage 2 and Stage 3 for temperatures of 116.9°C and 99.6°C the salt concentration is 5070 ppm and 6080 ppm, respectively.

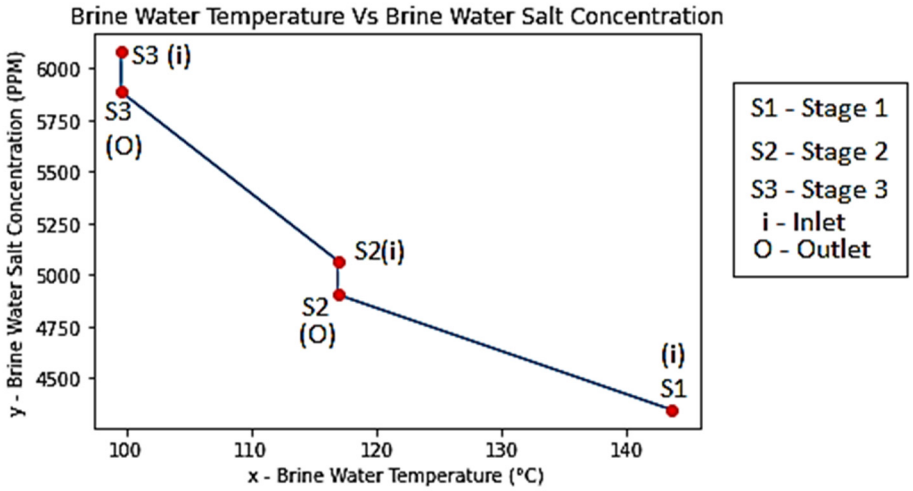


FIGURE 12: Brine water temperature vs brine salt concentration

According to the United States Geological Survey (USGS), water can be categorised into four groups (Dieter et al., 2017). These are freshwater with salt concentration of 1000 ppm or less, slightly saline water with salt concentration of 1000 - 3000 ppm, moderately saline water with salt concentration of 3000 - 10000 ppm and highly saline water with salt concentrations of 10000 - 35000 ppm. Salt concentration also influences the production of distilled water and the temperature of the distilled water affects its salt concentration as shown in Figure 13. The salt concentration in distilled water decreases if its temperature increases. At Stage 1 at a temperature of 143.5°C the salt concentration is 142 ppm, whereas at Stage 2 and Stage 3 at temperatures of 116.9°C and 99.6°C the salt concentration is 164 ppm and 194 ppm, respectively. Hence, the distilled water obtained from the integrated solar MSF distilled geothermal system is of high quality.

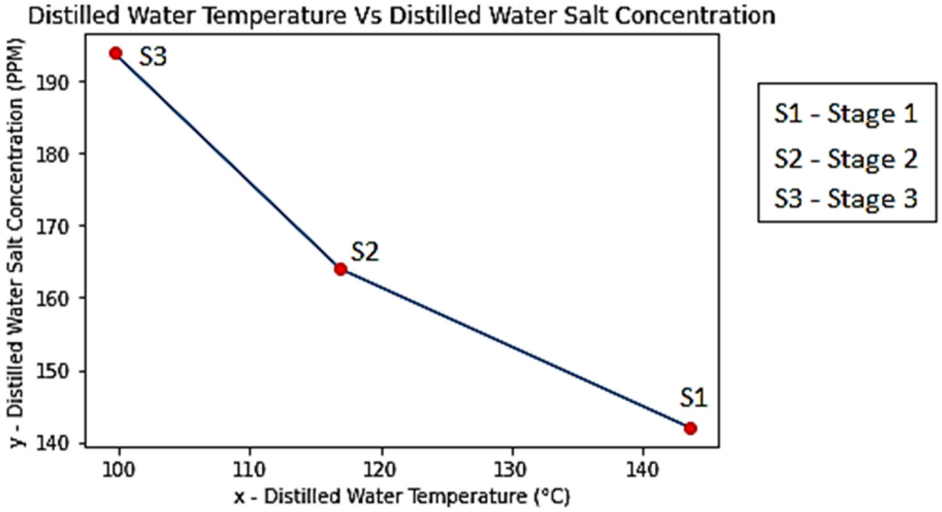


FIGURE 13: Distilled water temperature vs distilled water salt concentration

Figure 14 depicts the salt concentration based on the mass flowrate and temperature variation of geothermal water entering stage 1 after the solar collector. It has been observed that the salt

concentration increases if the temperature in the brine chamber increases, it decreases, however, in the evaporation chamber.

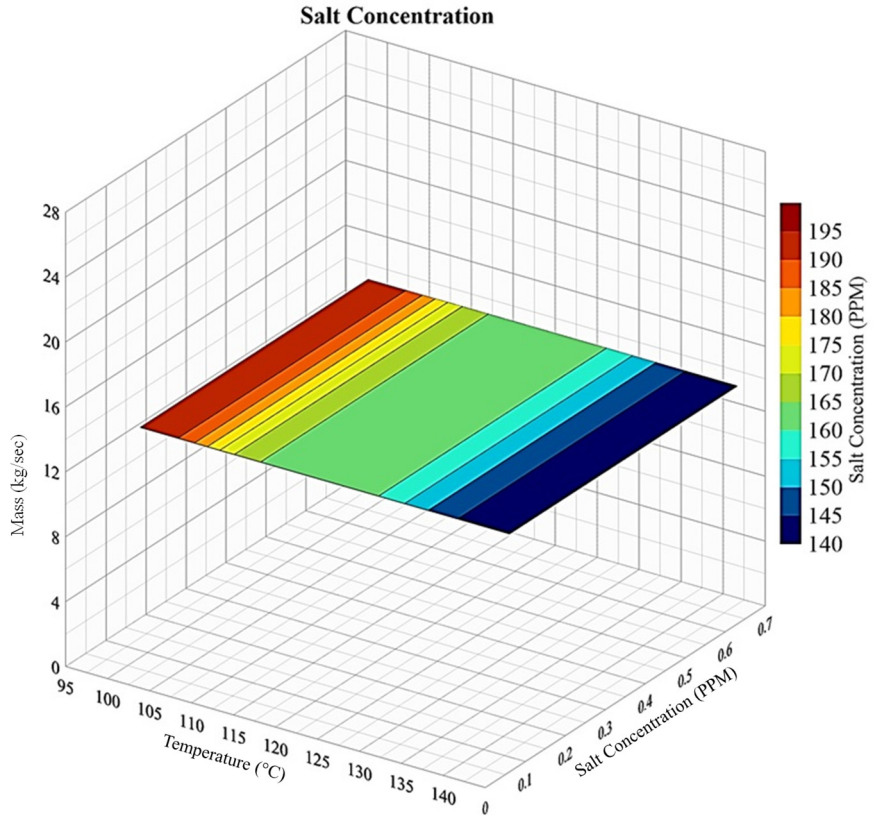


FIGURE 14: Salt concentration based on mass and temperature variation

At the same time, the mass flow rate decreases with increasing temperature in the brine and the evaporation chamber at each stage. Figure 15 represents the mass flow rate based on the enthalpy and temperature variation.

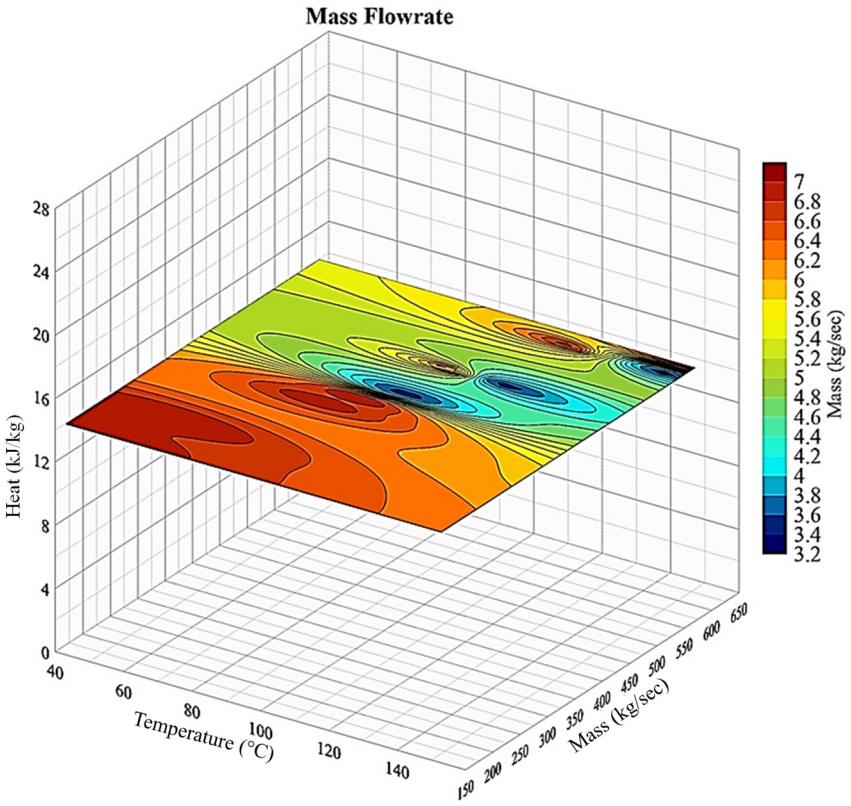


FIGURE 15: Mass flow-rate based on heat and temperature variation

### 5.2 Cost analysis

The numbers presented in Table 7 are simple estimates of the expenditure and may change based on technology accessibility in the area. Geothermal salt separation is a very effective method because it is operated by differences in temperature and their thermodynamical states, with no physical or moving parts. As a result, the energy source accounts for a large portion of the technique's operational expenses rather than the process itself. To warm the geothermal water for the fractional distillation, hydrocarbon fuels are usually employed. However, in our case we are using solar collectors to enhance the temperature of the geothermal water which will reduce the cost of electricity. Whenever renewable resources like geothermal power are combined with a desalination system, capital costs can be drastically reduced.

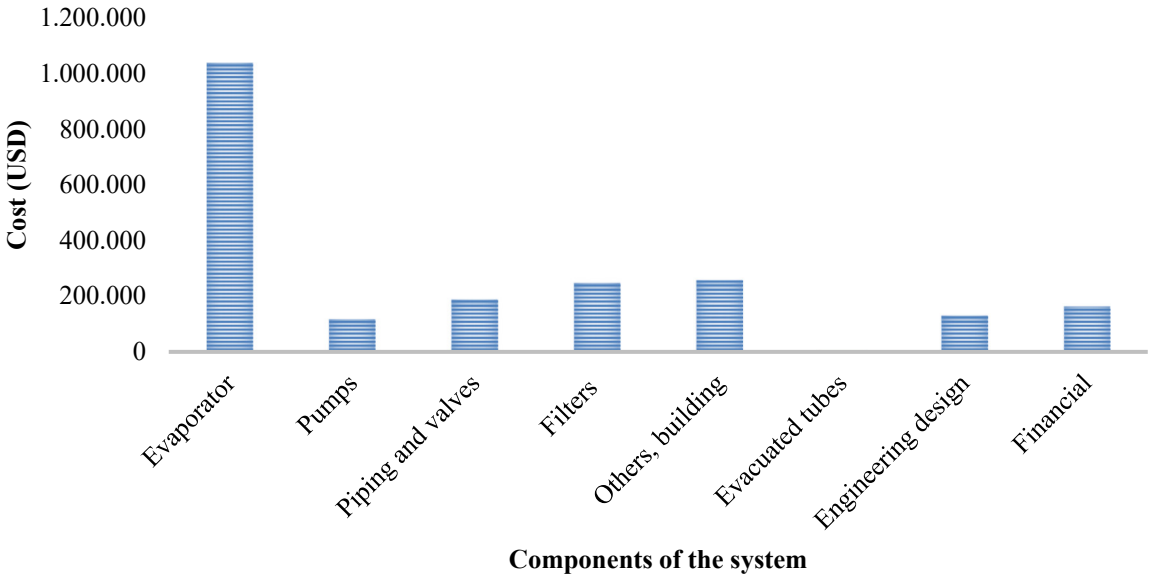


FIGURE 16: CAPEX cost analysis of the solar MSF geothermal desalination system

The CAPEX and OPEX cost assessment of the solar MSF geothermal desalination process is shown in Table 7. Filters, pumps, evaporators, valves, and pipework are already included in the cost of hardware. Indirect expenditures such as structural engineering, constructing infrastructure, and project development are included. CAPEX has a total cost of roughly 0.064 US$/m$^3$ (Figure 16).

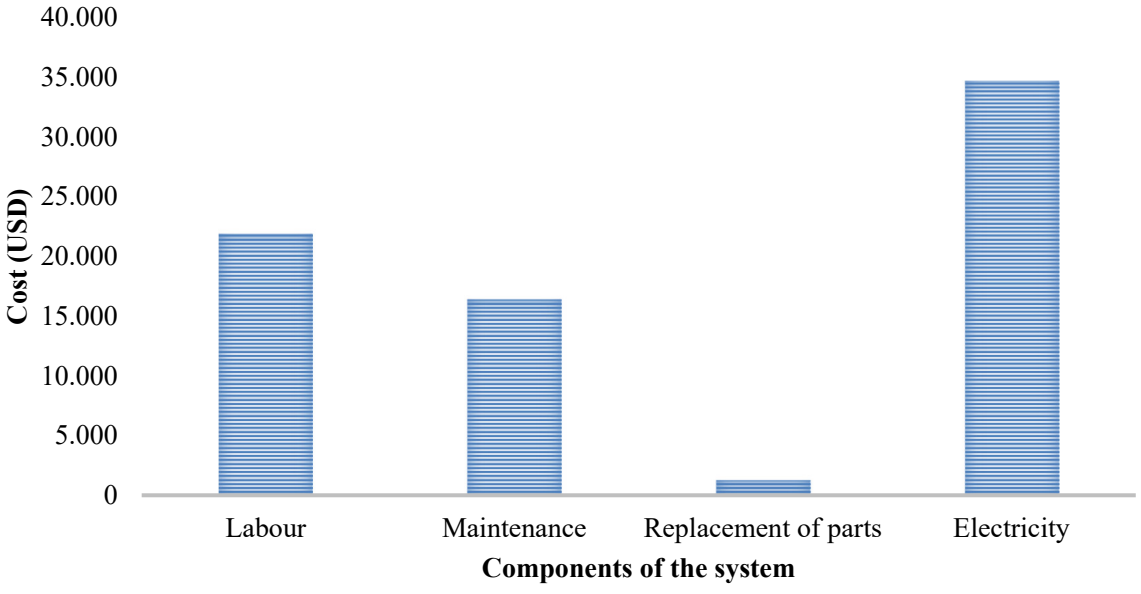


FIGURE 17: OPEX cost analysis of the solar MSF geothermal desalination system per year

TABLE 7: Cost analysis of solar MSF geothermal desalination system

| **Particulars** | **Cost in US$** | **Cost in US$/m$^3$** |
|---|---|---|
| Evaporator | 1,040,551 | |
| Pumps | 118,026 | 0.007 |
| Piping and valves | 188,939 | 0.011 |
| Filters | 249,015 | 0.014 |
| Others, building | 258,803 | 0.015 |
| Evacuated Tubes | 1,225 | |
| Engineering design | 131,455 | 0.008 |
| Financial | 164,319 | 0.010 |
| ***Subtotal*** | ***2,152,333*** | ***0.064*** |
| **OPEX** | | |
| **Particulars** | **Cost in US$/year** | **Cost in US$/m$^3$** |
| Labour | 21,909 | 0.012 |
| Maintenance | 16,431 | 0.009 |
| Replacement of parts | 1,305 | 0.001 |
| Electricity | 34,740 | 0.018 |
| ***Subtotal*** | ***74,385*** | ***0.039*** |
| ***Total*** | ***2,226,718*** | ***0.103*** |

Table 7 also shows the operational cost of the solar MSF geothermal desalination system which includes labour, O&M, replacement unit cost and electricity (Figure 17). The analysis showed that the cost of electricity represents the highest part of the total OPEX, the specific operational cost is 0.0566 US$/m$^3$. The calculated unit cost is around 0.103 US$/m$^3$ (Table 7).

## 6. CONCLUSIONS

As Dholera has been declared to be a smart city, its government is taking smart development seriously. Smart cities are technologically modern cities that utilize several types of sensors, electronic methods, and voice activation techniques for data collection. Potable drinking water is an issue which needs to be taken care of in this regard. For the same reason, the development plan for Dholera Special Investment Region (Dholera SIR) is considering the tapping of the Narmada canal as a prime source of water. However, this process will take some time to be implemented. Taking this issue into consideration, the author of this report has designed an integrated solar MSF geothermal desalination system. The system is a green facility involving a fully sustainable operation. There were four major aims of the report, namely to develop a thermodynamic model for a solar evacuated tubes system according to the need of a Multi-Stage Distillation system, to develop a thermodynamic model for the Multi-Stage Distillation system for geothermal water desalination, to simulate the production of heat from an evacuated tube solar collector with the geothermal Multi-Stage Distillation system to separate steam and salt and to perform a cost analysis of the system. Geothermal water temperature, flow rate, separation temperature, pressure and salinity were used as design parameters. This system will act as a co-generation system for the production of freshwater, salt and heat. The result of the simulation indicates that the salt concentration of the geothermal water will be reduced from 4210 ppm to 142 ppm. The quantity of freshwater obtained from the system will be 0.9 kg/s. The cost estimation of the system was done based on CAPEX and OPEX parameters. The total cost of the system is around 223 kUSD. The price of water per cubic meter is estimated to be around 0.103 USD. The whole system is green and reliable, however,

there is a lot of residual heat which is being wasted. This heat can be used for direct application purposes like food drying, milk pasteurization, etc.

## ACKNOWLEDGEMENTS

First, I would like to thank GRÓ GTP and the Centre of Excellence for Geothermal Energy, Pandit Deendayal Energy University, for giving me the opportunity for training in Iceland. I would also like to acknowledge Dr. Maria Gudjonsdottir and Dr. Pall Valdimarsson for supervising me in this project. I am also grateful to Dr. Gudni Axelsson, Ms. Frida Omarsdottir and other staff of GRÓ GTP for their support and assistance. I would also like to thank Prof. Anirbid Sircar for his guidance and support.

## NOMENCLATURE

$Q_{absorber}$ = Heat absorbed (kJ)
$A_{collector}$ = Area of collector ($m^3$)
$l_{intensity}$ = Intensity of solar radiation ($W/m^2$)
$n_{optical}$ = Optical efficiency (%)
$d$ = Diameter of evacuated tube (mm)
$l$ = Length of evacuated tube (mm)
$n$ =Number of evacuated tubes
$Q_{loss}$ =Heat loss (kJ)
$F_{heat\ loss}$ = Heat loss factor
$S_{collector}$ = Solar energy on collector ($W/m^2$)
$U_{Loss}$ = Heat loss coefficient ($W/(m^2K)$)
$T_{inner}$ = Inner temperature of evacuated tube (°C)
$T_{average}$ = Average temperature of evacuated tube (°C)
$Q_{useful}$ = Useful heat (kJ)
$H_{absorbed}$ = Heat absorbed by evacuated tube (kJ)
$\Delta T$ = Temperature difference at each stage (°C)
$T_{flash}$ = Temperature of flash (°C)
$T_{brine}$ = Temperature of brine (°C)
$T_1$ = Temperature at stage 1 (°C)
$T_{j+1}$ = Temperature at stage j+1 (°C)
$\dot{m}_{distilled}$ = Mass flow of distilled water (kg/s)
$l_{heat}$ = Sensible latent heat (J)
$\dot{m}_{recoverable}$ = Mass flow of recoverable brine water (kg/s)
$C_p$ = Specific heat of water (J/kg°C)
$X_{distilled}$ = Salt concentration of distilled water (ppm)
$x_{flash}$ = Salt concentration of flash water (ppm)
$x_{brine}$ = Salt concentration of brine water (ppm)
$\dot{m}_{flash}$ = Mass flow of flash water (kg/s)
$\dot{m}_{steam}$ = Mass flow of steam (kg/s)
$\dot{Q}$ = Heat transfer (W)
$h_j$ = Specific enthalpy at stage j (kJ/kg)
$h_{j+1}$ = Specific enthalpy at stage j+1 (kJ/kg)
$T_{ambient}$ = Ambient temperature (°C)
$CAPEX$ = Capital Expenditures (US$)
$n1$ = Number of years
$i$ = Interest rate (%)
$OPEX$ = Operational expenditures (US$)
LP Steam = Low pressure steam (bar)

## REFERENCES

Abdul Nasser A., and Mabrouk, H.E.S., 2010: Steam, electricity, and water costs evaluation of power-desalination co-generation plants. *Desalin. and Water Treatment, 22,* 56–64.

Aghil, T.B., Mohna, K., Srinivas, Y., Rahul, P., Paul, J., Alby, E.R., Nair, N.C., and Chandrasekar, N., 2014: Delineation of electrical resistivity structure using Magnetotellurics: a case study from Dholera coastal region, Gujarat, India. *J. Coast. Sci., 1 (1),* 41e46.

Al-Hallaj, S., Farid, M.M., and Tamimi, A.R., 1998: Solar desalination with a humidification-dehumidification cycle: Performance of the unit. *Desalination, 120,* 273–280.

Al-Shammiri, M., and Safar, M., 1999, Multi-effect distillation plants: state of the art. *Desalination, 126,* 45–59.

Amio Water Treatment Ltd., 2021: *AMIO Water Technology.* website: *http://www.amiowater.com/technology*.

Arshad, HK., 1986: *Desalination processes and multistage flash distillation practice.* Elsevier Science Publishers, 596 pp.

ASHRAE, 1995: *Handbook of HVAC Applications,* Atlanta, NY 713 pp.

Ayyash, Y., Imai, H., and Yamada, T., 1994, Performance of reverse osmosis membrane in Jeddah Phase I plant. *Desalination, 96,* 215–224.

Biswas, S.K., 1987: Regional tectonic framework, structure and evolution of the western marginal basins of India. *Tectonophysics, 135,* 307–27.

Bremere, I., Kennedy, M., Stikker, A., and Schippers, J., 2001: How water scarcity will a ect the growth in the desalination market in the coming 25 years. *Desalination, 138,* 7–15.

Buros, O.K., 2000: *The ABCs of Desalting, 2nd edn*. ASIN: B0006S2DHY, International Desalination Association.

Caldera, U., and Breyer, C., 2017: Learning curve for seawater reverse osmosis desalination plants: Capital cost trend of the past, present, and future. *Water Resour. Res., 53,* 10523–10538.

Coris, R., 1986: Scaling and corrosion in geothermal equipment: problems and preventive measures, *Geothermics, Elsevier, 15*, 839.

Dieter, C.A., Linsey, K.S., Caldwell, R.R., Harris, M.A., Ivahnenko, T.I., Lovelace, J.K., Maupin, M.A., and Barber, N.L., 2017, Estimated use of water in the United States county-level data for 2015: *U.S. Geological Survey data release, https://doi.org/10.5066/F7TB15V5*.

Eltawil, M.A., Zhengming, Z., and Yuan, L., 2008: Renewable energy powered desalination systems: technologies and economics- state of art, *Proceedings in Twelfth International Technology Conference, IWTC12 2008, Alexendria, Egypt,* 1099.

European Geothermal Energy Council, 2010: *The voice of geothermal industry in Europe*. Renewable Energy House: Brussels, Belgium. *Available online: http://www.egec.org/.*

Fath, M.E.S., 1998: Solar desalination: A promising alternative for water provision with free energy, simple technology and a clean environment. *Desalination, 116,* 45–56.

Gao, H., Jiang, A., Huang, Q., Xia, Y., Gao, F., and Wang, J., 2020: Mode-Based Analysis and Optimal Operation of MSF Desalination System. *Processes,* 8, 1-22.

Hamed, O., Mustafa, G.M., and BaMardouf, K., 2001: Prospects of improving energy consumption of the multi-stage flash distillation process. *In: Proceedings of the Fourth Annual Workshop on Water Conservation in Dhahran the Kingdom of Saudi Arabia,* 14 pp.

Jones, E., Qadir, M., Van Vliet, M.T.H., Smakhtin, V., and Kang, S.M., 2019: The state of desalination and brine production: A global outlook. *Sci. Total Environ., 657,* 1343–1356.

Kalogirou, S.A., 2004: Solar thermal collectors and applications. *Progress in Energy and Combustion Science, 30,* 231-295.

Kalogirou, S., Eleftheriou, P., Lloyd, S., and Ward, J., 1994: Design and performance characteristics of a parabolic trough solarcollector system. *Appl Energy, 47,* 341–54.

Khawaji, A.D., Kutubkhanah, I.K., and Wie, J.M.A., 2007: MGD seawater RO desalination plant for Yanbu Industrial City. *Desalination, 203,* 176–88.

Liu, D.B., and Su, Y.Y., 2007: Challenges in global water resource management. *Express Water Resour. & Hydropower Inf., 2,* 3–8.

Mahmoudi, H., Abdul-Wahab, S.A., Goosen, M.F.A., Sablani, S.S., Perret, J., and Ouagued, A., 2008: Weather data and analysis of hybrid photovoltaic–Wind power generation systems adapted to a seawater greenhouse desalination unit designed for arid coastal countries. *Desalination, 222,* 119–127.

Mahmoudi, H., Spahis, N., Goosen, M.F.A., Ghaffour, N., Drouiche, N., and Ouagued, A., 2010: Application of geothermal energy for heating and freshwater production in a brackish water greenhouse desalination unit: A case study from Algeria. Renew. *Sustain. Energy Rev., 14,* 512–517.

Mathioulakis, E., Belessiotis, V., and Delyannis, E., 2007, Desalination by using alternative energy: review and state-of-the-art. *Desalination, 203,* 346–65.

Merh, S., 1995: *Geology of Gujarat*. Banglore, Geological Society of India, 222 pp.

Miller, J., 2003: *Review of water resources and desalination technologies.* Materials Chemistry Department, Sandia National Laboratories, report, 54 pp.

Misra, A.A., Maitra, A., Sinha, N., Dey, S., and Mahapatra, S., 2019: Syn- to post-rift fault evolution in a failed rift: a reflection seismic study in central Cambay Basin (Gujarat), India. *International Journal of Earth Sciences, 108,* 1293-1316.

Owen, L.B., and Michels, D.E. 1948: *Geochemical engineering reference manual,* DOE/ SF/11520-T1, Salt Lake City, Utah, TerraTek report, 558 pp.

Raluy, R.G., Serra, L., and Uche, J., 2004: Life-cycle assessment of desalination technologies integrated with energy production systems. *Desalination, 167,* 445–58.

Rice, W., and Chau, D.S.C., 1997: Freeze desalination using hydraulic refrigerant compressors. *Desalination, 109,* 157–64.

Rodrıguez, G., Rodrıguez, M., Perez, J., and Veza, J., 1996: A systematic approach to desalination powered by solar, wind and geothermal energy sources. *In Proceedings of the Mediterranean Conference on Renewable Energy Sources for Water Production, Santorini, Greece*, 20–25.

Rognoni, M., La Dissalazione Dell'acqua, M., and Descrizione, A., 2010: *Valutazione Delle Principali Tecnologie, 1st ed.* Dario Flaccovio Editore s.r.l.: Palermo, Italy, ISBN 9788857900308.

Shah, M., Sircar, A., Sahajpal, S., Sarkar, P., Sharma, D., Garg, S., Mishra, T., and Shukla, Y., 2017: Geochemical analysis for understanding prospectivity of low enthalpy geothermal reservoirs of Dholera. *In: Proceedings, 42nd Workshop on Geothermal Reservoir Engineering. Stanford University, Stanford, California,* 1e16.

Sharma, N., 2013: *Physico-chemical characterization of the thermal spring waters occurring in Gujarat, India; 2013.* CEGE report, 1–16.

Shatat, M., and Riffat, S.B., 2014: Water desalination technologies utilizing conventional and renewable energy sources. *International Journal of Low- Carbon Technologies, 9,* 1-19.

Singh, V., Srivastava, A.K., Painuly, P.K. and Chandra, M., 2007: Neural networks and their applications in lithostratigraphic interpretation of seismic data for reservoir characterization. *The Leading Edge, Society of Exploration Geophysicists, 26(10),* 1244.

Strathmann, H., Winston, W.S., and Sirkar, K.K., 1992: *Membrane Handbook,* ISBN-0-442-23747-2. Van Nostrand Reinhold, 246–254.

Vaidya, D., Shah, M., Sircar, A., Sahajpal, S., and Dhale, S., 2015: Geothermal energy: exploration efforts in India. *Int. J. Latest Res. Sci. Technol., 4 (4),* 1e23.

Wang, H.T., Li, B.A., and Liu, B., 2014: The current situation of seawater desalination technology and new technology review. *J. Salt Sci. Chem. Ind., 6,* 1–5.

Wangnick, K., 2000: *IDA worldwide desalting plants inventory: report No. 16.* Produced by Wangnick Consulting for the International Desalination Association.

UN. ESCWA, 2001: *Water desalination technologies in the ESCWA member countries.* UN-ESSWA, ASIN: E/ESCWA/TECH/2001/3. United Nations, report, 177 pp.

Winston, R., 1974: Solar concentrators of novel design. *Solar Energy, 16,* 89–95.

Xu, T., 2005: Ion exchange membranes: State of their development and perspective. *J Membrane Sci, 263,* 1–29.

Yadav, K., and Sircar, A., 2019: Integrated 2D joint inversion models of gravity, magnetic, and MT for geothermal potentials: a case study from Gujarat, India. *Model. Earth Syst. Environ., 5,* 963–983.

Yadav, K., Sircar, A., Jani, D., Bist, N., Nirantare, A., Mali, N. and Singh, S., 2021: "Geochemical characterization of geothermal spring waters occurring in Gujarat, India", *International Journal of Energy and Water Resources, 5,* 391-404.

Zhang, B.Z., 2008: Multistage flash seawater desalination technology. *Cfhi Technol., 4,* 48–49.

Zhang, T., and Yang, H., Kalogirou, S.A., 2019: High efficiency plants and building integrated renewable energy systems. *Handbook of Energy Efficiency in Buildings,* 443-595.

Zhao, Z.H., Yuan, Y.C., and Chen, Y., 2017: Analysis of multi-stage flash seawater desalination technology. *Sci. Mosaic, 8,* 46–49.